INVESTIGATION OF PROPAGATION ACCURACY EFFECTS WITHIN THE MODELING OF SPACE DEBRIS

A. Horstmann and E. Stoll

Technische Universität Braunschweig, Institute of Space Systems, 38108 Braunschweig, Germany, Email: {andre.horstmann,e.stoll}@tu-braunschweig.de

ABSTRACT

ESA's Meteoroid And Space Debris Terrestrial Environment Reference (MASTER) allows to assess the debris and meteoroid flux imparted on a spacecraft in Earth orbit. In addition, spatial densities of artificial satellites in altitudes up to 1000 km above Geostationary Earth Orbit (GEO) can be evaluated. As of now, the most recent version is based on its reference population on 1st May 2009. This includes space debris with diameters down to d $\geq$ 1 µm.
This paper gives an insight to the accuracy influence of the implemented propagator and the resulting quantities which are reflected by the results of MASTER-2009 for the diameter spectrum of d $\geq$ 1 cm. The evaluation of spatial density calculations will reveal the impact of the underlying propagators with their different settings. Especially, the propagation in Low Earth Orbit (LEO) is significantly affected since the modelling of aerodynamic drag is strongly related to the decay rate, hence, the number of on-orbit objects. The impact on the space debris environment for two propagators using different atmosphere models will be shown.

1. INTRODUCTION

1.1. Overview

Modelling the space debris environment has a great influence on risk estimations for manned and and unmanned space missions. ESA's MASTER allows to assess the debris and meteoroid flux imparted on a spacecraft in Earth orbit up to altitudes of 36 786 km. In its current release of MASTER-2009, objects with diameters down to d $\geq$ 1 µm originating from various sources are considered [2]. The interaction of the space debris environment with operational payloads can result in collision avoidance maneuver, due to an increased collision risk, or even a complete or partial fragmentation of the spacecraft. A visualisation of the space debris environment for objects greater than 1 cm is shown in Fig. 1. The critical diameter spectrum of 1 cm to 10 cm is of special interest, because these objects are difficult to detect but can yield a complete disintegration of a satellite in the case of a collision [6]. Key aspects of the space debris modelling are the initial generation of fragmentation clouds and the propagation of large amounts of objects to assess future collision risks. The population prediction is performed with high efficiency propagators that are capable of considering different perturbations, such as geopotential, third bodies, solar radiation pressure and atmospheric drag. This paper gives an insight into the accuracy influence of the implemented propagator and the resulting quantities which are reflected by the results of MASTER-2009 for the diameter spectrum of d $\geq$ 1 cm. The results and conclusions will be based on the Fengyun-1C anti-satellite test along with the induced fragmentation cloud.

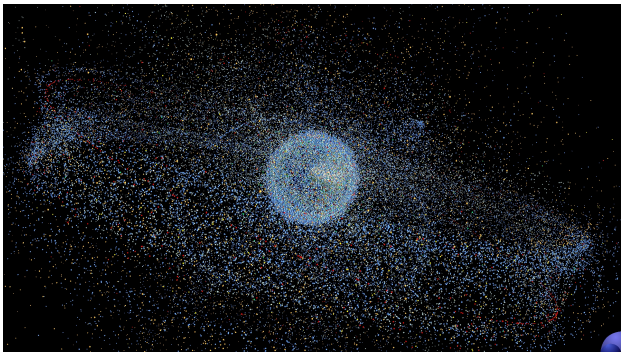

Figure 1: Visualisation of the space debris environment with objects greater than 1 cm in May 2009

1.2. Orbit propagation

Predicting the motion of satellites on orbits around celestial bodies is performed with orbit propagation. The underlying mathematical process to determine the time-dependent position of a satellite is performed with propagators. Regardless of the applied propagation method, the key properties are speed and accuracy. Propagation methods can generally be distinguished between three categories: Numerical, analytical, and semi-analytical. Numerical propagation is performed by direct integration of a given equation of motion and can yield most accurate results based on the underlying force model of the pertur-

bating forces. However, it comes with the cost of speed since the numerical integration requires a high computational effort. Analytical propagation makes use of mathematical formulations for the effects of the perturbations on the satellite. They work faster than numerical methods, however, have drawbacks when it comes to accuracy. One of the most well-known analytic propagation methods is SGP4 which can also be used to transform Two Line Elements (TLE) sets to mean Keplerian Elements [3, 7]. Semi-analytical models are usually used in long-term orbit predictions with analytic formulations for the change of orbital elements over time. The difference to the analytic method is that the underlying mathematical expressions are described more accurately but only for long periodic effects. These complex formulations then have to be integrated numerically, however with a much larger step sizes than the numerical integration due to the consideration of exclusively long-term effects.

Modeling the space debris environment is heavily relying on orbit propagation since it provides spatial distributions of millions of objects in space over a long period of time. The population of objects has to be dynamically modeled and propagated afterwards. In order to keep the computational effort manageable, semi-analytical propagators are chosen to provide a trade-off between speed and accuracy of the propagation. However, even the selection of the underlying semi-analytical propagator can yield different results in terms of object population which is due the complexity and accuracy of the considered mathematical formulations for the perturbating forces.

One particular example is the consideration of an accurate atmosphere model. Calculating the induced atmospheric drag in lower altitudes is based on the air density in the corresponding altitude. Especially small objects and objects with a high area-to-mass ratio are greatly affected be the atmospheric drag which results in an increased decay rate for these objects over time. Since the early 1960's, atmospheric models are developed and continuously maintained to provide the most accurate air density values (Fig. 2). Some of the most well-known are Cospar International Reference Atmosphere (CIRA), King-Hele or Mass Spectrometer - Incoherent Scatter (MSIS) which provide air density tables dependent on altitude, solar and geomagnetic activity or non-tabled mathematical formulations, e.g. exponential functions to describe the air density dependent on altitude and solar activity.

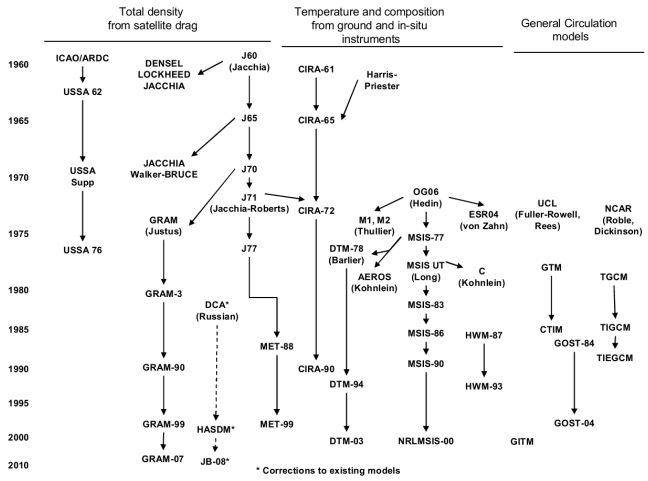

Figure 2: Development of atmosphere models [8]

The consequence of selecting a different atmosphere models for the propagation of the same fragmentation event is evaluated in the next chapters.

2. SELECTED PROPAGATORS

Two different propagators are used for the comparison which are designed to process a very high number of objects by using a semi-analytic approach for deriving orbital elements (Table 1). Although there are propagation techniques that rely on numerical propagation of the osculating elements, these methods require extensive computation time when being applied to a large amount of objects. To keep the computational effort in manageable boundaries, semi-analytic methods pose an alternative to the numerical propagation with acceptable accuracy. The difference between both propagators is the underlying atmospheric model. For P_1, MSIS-77 is used to provide air density values to calculate the induced drag, where in P_2 the most recent version NRLMSISE-00 is used. Since both propagators are designed to propagate a high number of objects, only geopotential terms with long-periodic secular contribution are considered (cp. Sec. 1.2). Although P_2 is additionally considering the zonal J_6-term, the orbit perturbations in lower altitudes is dominated by atmospheric drag. This is where the atmospheric model plays a major role, especially in the decay rate and consequently in the spatial density.

Table 1: Propagator settings

Propagator	P1	P2
Geopotential	J_2, J_4	J_2, J_4, J_6
Atmosphere model	MSIS-77 (oblate)	NRLMSISE-00
Sun gravity	on (n=3)	
Moon gravity	on (n=3)	
Solar radiation pressure	on	

The induced acceleration due to aerodynamic drag can be calculated with [8]:

$$\vec{a} = -\frac{1}{2} \cdot \frac{C_D A}{m} \cdot \rho \cdot v_{rel}^2 \cdot \frac{\vec{v}_{rel}}{|\vec{v}_{rel}|}. \qquad (1)$$

C_D is the drag coefficient which is usually set to approximately 2.2 , A is the projected area in flight direction, m is the object mass, v_{rel} the relative velocity, and ρ the air density provided by the atmosphere model. The MSIS models provide air density values usually dependent of altitude, solar and geomagnetic activity. As reflected by Eq. 1, a more dense air density leads to a higher negative acceleration, hence reducing the semi-major axis of

the considered object. ESA's MASTER is able to evaluate objects with a perigee down to 186 km. Below the objects contribution to the spatial density is omitted.

In the following chapters, the influence of choosing a different atmosphere model for the propagation of fragmentation clouds is evaluated.

3. INITIAL CLOUD GENERATION

The Fengyun-1C anti-satellite test was performed on January 11, 2007. The 880 kg weather satellite Fengyun-1C was deliberately destroyed in a sun-synchronous orbit of 860 km by an Exoatmospheric Kill Vehicle (EKV). Due to the high impact velocity of 7 km s^{-1} to 8 km s^{-1}, the satellite was completely disintegrated making it the most catastrophic fragmentation event in terms of detected object numbers since the beginning of the space age in the 1950's. A visual approximation of the fragmentation cloud is given in Fig. 3. Shortly after the event, the cloud

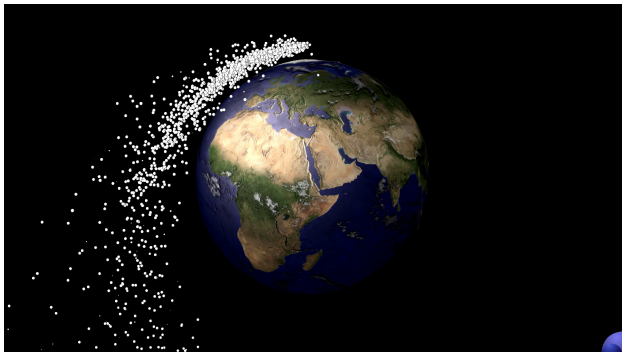

Figure 3: Initial Fengyun-1C cloud one hour after the event.

forms a band due to the different orbital velocities induces by the high energy impact. Modelling the diameter distribution of this catastrophic event was performed by following the power law from within the NASA breakup model which is shown in Fig. 4 [5]. As of February 2017, the Space Surveillance Network (SSN) has catalogued 3438 objects bigger than approximately 10 cm and are related to the Fengyun-1C event. The evaluation of the resulting spatial density contribution in LEO for different diameter spectra is shown in Fig. 5.

Looking at the d $\geq$ 10 cm fragments (blue line), there is a peak in spatial density at around 850 km, which indicates the fragmentation altitude of the Fengyun-1C anti-satellite test. The Δv-distribution for all generated fragments, which is due to the impact of the EKV, changes the orbital elements for the fragment population which results in spatial object contribution in lower and higher altitudes. Consequently, this generates a decreasing spatial density trend for increasing altitude difference. These objects were displaced from the initial satellite orbit and contribute to the spatial density spectrum in a broader range of altitude. The same trend is observable for the

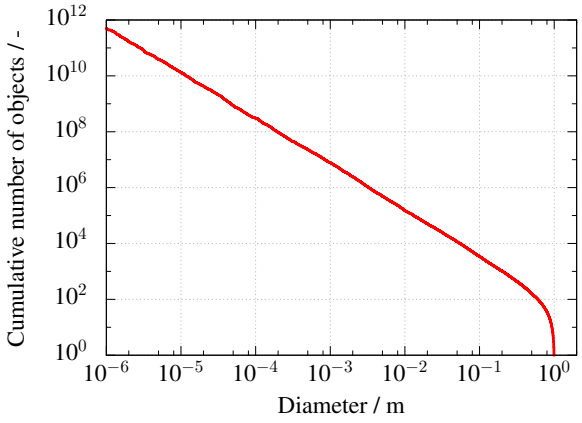

Figure 4: Initial Fengyun-1C cumulative object distribution following the NASA breakup model

other diameter spectrum shown in Fig. 5. Due to the logarithmic axis, the trend seems to decrease for lower diameter thresholds, however it is consistent in terms of spatial density difference. The shift in magnitude of spatial density for the different diameter spectra is due to the cumulative diameter distribution shown in Fig. 4.

4. CLOUD PROPAGATION AND EVALUATION

After modelling the initial cloud and therefore, also the initial spatial density distribution, both propagation methods (cp. Sec. 2) are used to propagate each fragment individually. Over time, the spatial distribution of the Fengyun-1C cloud evolves and due to the acting perturbations such as geopotential, third bodies, solar radiation pressure and atmospheric drag, the orbital elements of each individual fragment changes independently. This leads to a near equal distribution ob objects in proximity of the fragmentation altitude (cp. Fig. 6). This results in a change in spatial density distribution which is shown in Fig. 7 for the d $\geq$ 1 cm diameter spectrum. The initial cloud was propagated from 2007 to 2009 with the

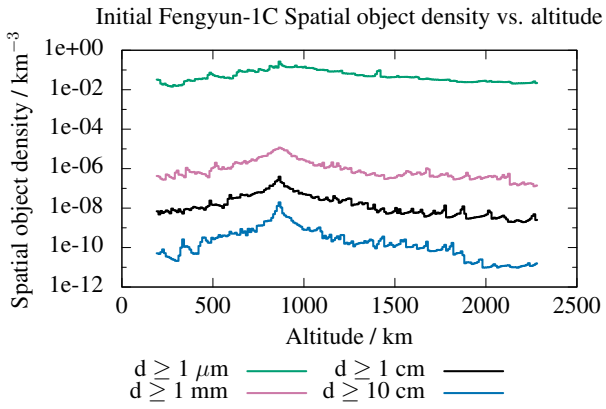

Figure 5: Initial Fengyun-1C spatial density distribution

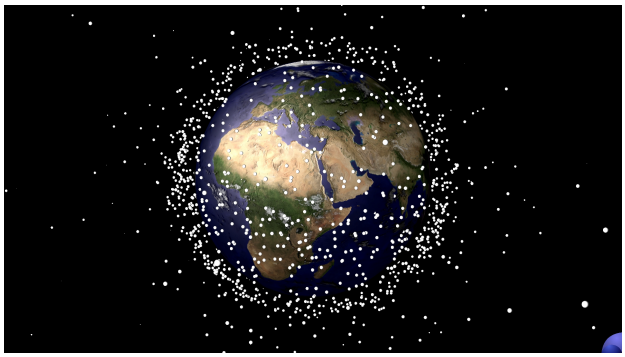

Figure 6: Fengyun-1C cloud two years after the event.

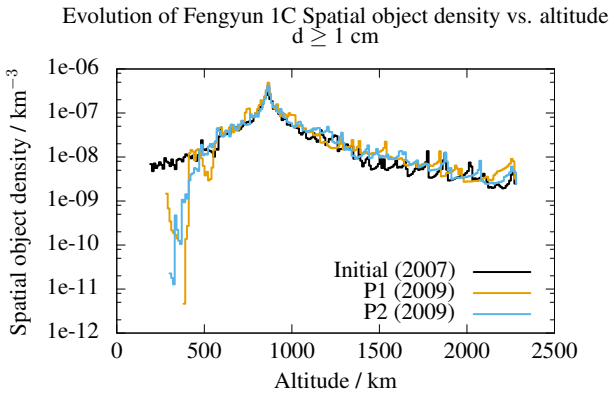

Figure 7: Fengyun-1C spatial density distribution evolution for the two different propagators

two different propagators which were described briefly in Table 1. The results of both propagators for the spatial density distribution two years later are shown in the same figure. The evaluations show that for both propagation methods, the spatial object density contribution is similar in the upper atmosphere, i.e. in altitudes above 600 km. Below 600 km, the results begin to deviate and show major differences. Investigating the relative deviation or "Error ratio" Δ gives a more detailed insight into this difference. The Error ratio is calculated by

$$\Delta = \frac{D_{P2} - D_{P1}}{D_{P2}}, \tag{2}$$

where D is the spatial object density for the corresponding propagation method $P1$ or $P2$. The results is shown in Figure 8.

The Error ratio drops from around zero to almost -14 in altitudes around 270 km. In higher altitudes, i.e. above 600 km, the natural decay is a minor effect since the air density is significantly lower and is therefore not acting on these objects to reduce the semi-major axis sufficiently.

The cumulative object numbers can highlight an important aspect and can show another perspective for the estimation of the induced errors by using different propagators (cp. Figure 9).

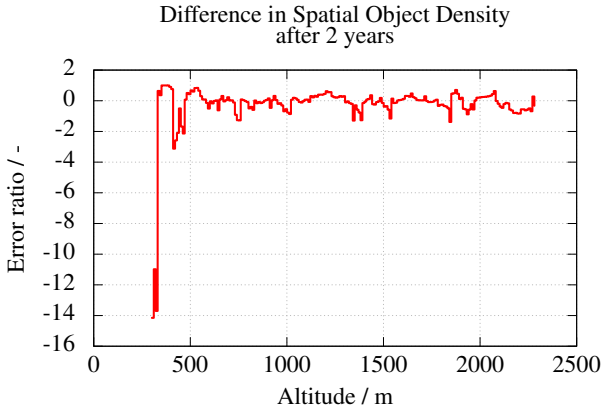

Figure 8: Difference in spatial density for the Fengyun-1C cloud between both integration methods

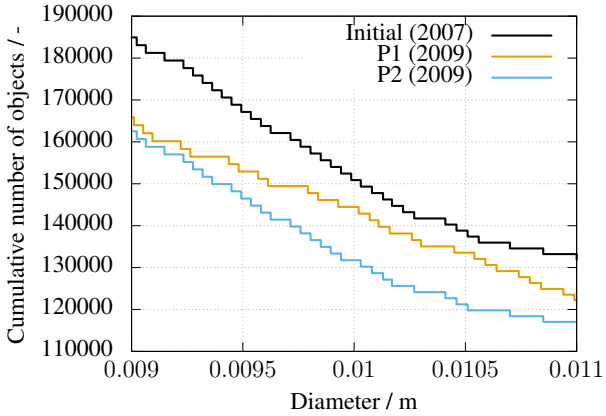

Figure 9: Fengyun-1C cumulative object number distribution for the two different propagators

Compared to the initial situation, both propagators show a decreased number of objects throughout the whole diameter spectrum which is due to the natural decay. However, at d $\geq$ 1 cm, there is a number difference of almost 9 % between the results of P1 and P2, using MSIS-77 and NRLMSISE-00, respectively.

5. CONCLUSIONS

The spatial object density in LEO and consequently the number of fragments in orbit, is not only dependent on the amount of fragmentations but also sensitive to the propagation method of individual cloud. Objects larger than 10 cm in diameter usually can be tracked in LEO which enables a continuous verification for these objects. The contribution of smaller objects has to be modelled using fragmentation models and accurate propagation methods and therefore relies on accurate propagation. The propagation effect has a yield significant differences in altitudes below 600 km, which includes the ISS Orbit as well as highly eccentric orbits. Since mul-

tiple other fragmentations are modelled, the effect is of cumulative nature which requires sophisticated propagation methods along with continuous maintenance and validation procedures in order to provide an accurate space debris population. Collision risk estimations which are based on the spatial object density, i.e. flux-based approaches, can be highly susceptible to accurate modelling of space debris [4]. Also space debris models such as ESA's MASTER are directly affected by accurate orbit prediction which makes continuous maintenance of current atmosphere models and investigation of new ways to obtain air density values a must for modelling the space debris environment [1, 2].

REFERENCES

1. Flegel, S. (2011). Maintenance of the ESA MASTER model. Technical report, Institut fr Luft- und Raumfahrtsysteme.
2. Horstmann, A., Wiedemann, C., Stoll, E., Braun, V., and Krag, H. (2016). Introducing upcoming enhancements of ESA's MASTER. In *AIAA Space 2016*, September 13 - 16, 2016, Long Beach, CA.
3. Kelso, T. (2007). Validation of sgp4 and is-gps-200 against gps precision ephemerides (aas 07-127). *Advances in the Astronautical Sciences*, 127(1):427.
4. Klinkrad, H. (2006). *Space debris - Models and Risk analyis*. Springer.
5. Liou, J. C. (2011). Orbital debris quarterly news. Technical Report 15/4, NASA.
6. Radtke, J., Kebschull, C., and Stoll, E. (2017). Interactions of the space debris environment with mega constellations-Using the example of the OneWeb constellation. *Acta Astronautica*, 131:55–68.
7. Vallado, D. and Crawford, P. (2008). Sgp4 orbit determination. In *AIAA/AAS Astrodynamics Specialist Conference and Exhibit*, page 6770.
8. Vallado, D. and McClain, W. (2013). *Fundamentals of Astrodynamics and Applications*. Space Technology Library.